Dark ice chemistry in interstellar clouds

Qasim, D.N.

Surface formation of methane in interstellar clouds

Methane is one of the simplest stable molecules that is both abundant and widely distributed across space. It is thought to have partial origin from interstellar molecular clouds, which are near the beginning of the star formation cycle. Observational surveys of CH_4 ice towards low- and high-mass young stellar objects showed that much of the CH_4 is expected to be formed by the hydrogenation of C on dust grains, and that CH_4 ice is strongly correlated with solid H_2O. Yet, this has not been investigated under controlled laboratory conditions, as carbon-atom chemistry of interstellar ice analogues has not been experimentally realized. In this study, we successfully demonstrate with a novel C-atom beam implemented in an ultrahigh vacuum apparatus the formation of CH_4 ice in two separate co-deposition experiments: C + H on a 10 K surface to mimic CH_4 formation right before H_2O ice is formed on the dust grain, and C + H + H_2O on a 10 K surface to mimic CH_4 formed simultaneously with H_2O ice. We confirm that CH_4 can be formed by the reaction of atomic C and H, and that the CH_4 formation rate is 2 times greater when CH_4 is formed within a H_2O-rich ice. This is in agreement with the observational finding that interstellar CH_4 and H_2O form together in the polar ice phase, i.e., when C- and H-atoms simultaneously accrete with O-atoms on dust grains. For the first time, the conditions that lead to interstellar CH_4 (and CD_4) ice formation are reported, and can be incorporated into astrochemical models to further constrain CH_4 chemistry in the interstellar medium and in other regions where CH_4 is inherited.

3.1 Introduction

Interstellar methane (CH_4) ice has been detected towards low- and high-mass young stellar objects (YSOs), where it has an abundance relative to H_2O ice of 1-11% (Boogert et al. 2015), and is observationally constrained to be formed primarily from the reaction of H-atoms and solid C at the onset of the H_2O-rich ice phase of molecular clouds (Öberg et al. 2008). This primary pathway to

D. Qasim, G. Fedoseev, K.-J. Chuang, J. He, S. Ioppolo, E.F. van Dishoeck, and H. Linnartz, *An experimental study of the surface formation of methane in interstellar molecular clouds*, Nat. Astron. (2020) in press 10.1038/s41550-020-1054-y

CH_4 ice formation is also accounted for in astrochemical models (Aikawa et al. 2008). Such a constraint is complemented by the fact that the sequential solid-state reactions, C + H → CH, CH + H → CH_2, CH_2 + H → CH_3, CH_3 + H → CH_4, are likely to be barrierless (Cuppen et al. 2017) and exothermic (Nuth III et al. 2006), whereas the gas-phase CH_4 formation pathway includes rate-limiting steps (Smith 1989). CH_4 has been detected on comets (Mumma et al. 1996; Gibb et al. 2003), which are thought to have delivered interstellar CH_4 to planetary bodies, particularly during the early phases of our Solar System. Indeed, CH_4 has been detected in a number of planetary systems (Formisano et al. 2004; Swain et al. 2008; Stern et al. 2015), where its origin may be from the interstellar medium (ISM), as reported for the CH_4 found in Titan's atmosphere (Mousis et al. 2002, 2009). In essence, CH_4 is a ubiquitous species within the star formation cycle, with partial origin from the ISM.

To date, the solid-state formation of CH_4 by atomic C and H under conditions relevant to the H_2O-rich ice phase in interstellar clouds has not been confirmed in the laboratory, which causes ambiguity to the idea of the origin and interstellar formation of CH_4. Experimental investigations have been limited to the hydrogenation of graphite surfaces (Bar-Nun et al. 1980) and H_2O-poor conditions (Hiraoka et al. 1998), where the reported formation pathways of CH_4 are still under debate. The work by Hiraoka et al. (1998), which the experimental conditions are closest to the study presented here, consisted of plasma-activated CO gas as the atomic carbon source and did not include a H_2O ice matrix. The present work shows CH_4 formation starting directly from atomic C in a H_2O-rich ice, which is a more realistic interstellar scenario. The lack of experimental evidence on this topic is due to the technical challenges that are associated with the coupling of an atomic carbon source with an ultrahigh vacuum (UHV) setup that is designed to study atom-induced surface reactions under molecular cloud conditions. In this study, we investigate two interstellar relevant reactions for CH_4 ice formation: the simultaneous deposition of C + H and C + H + H_2O on a 10 K surface. This first experimental investigation of CH_4 ice by the reaction of C- and H-atoms under conditions mimicking those of interstellar molecular cloud environments is essential to understanding the distribution of CH_4 in the star formation cycle. Such work also provides formation yields, rates, temperature and reactant dependencies – values which were not previously available in the literature.

3.2 Results

Figure 3.1 provides a visual of the two investigated experiments, whereas more details are found in the Methods section. Product identification is unambiguously shown by the *in situ* detection technique, reflection-absorption infrared spectroscopy (RAIRS). A list of the experiments performed and the following formation yields are provided in Table 3.1. The flux of H_2O ($\sim 6 \times 10^{12}$ molecules cm^{-2} s^{-1}) was chosen to create a CH_4:H_2O ratio of 10% for experiments 2.1-2.3 in order to reflect the composition of interstellar ices (Boogert et al. 2015). It is important to note that H_2O is simultaneously deposited with C and H to create a mixed CH_4 and H_2O ice, as would be found in cold interstellar clouds, and is not meant to represent the accretion of gas-phase H_2O in such environ-

ments. The flux of H-atoms used was $\sim 9 \times 10^{12}$ atoms cm^{-2} s^{-1}, in comparison to $\sim 5 \times 10^{11}$ atoms cm^{-2} s^{-1} for that of C-atoms, which is representative of the dominance of H-atoms over C-atoms in the ISM. Each experimental set has the purpose of disentangling other possible CH_4 formation routes. Additionally, the table provides information on how various experimental conditions influence the formation of CH_4 (CD_4) when H_2O is present and/or absent. The results from each experiment are discussed below.

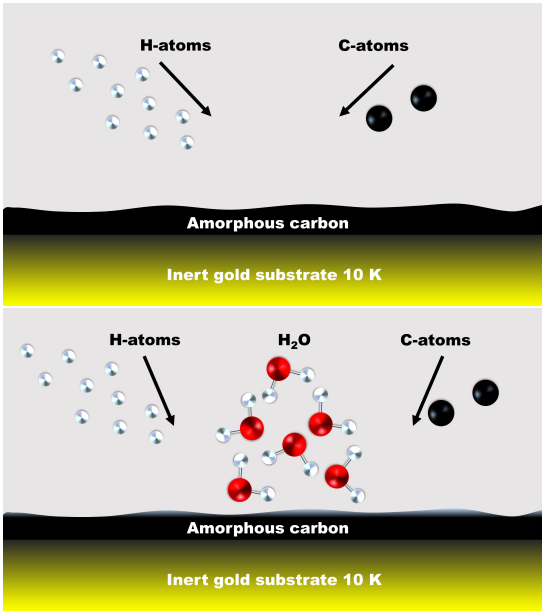

Figure 3.1: Visualization of the two experiments highlighted in this study. (Left) The simultaneous deposition of C- and H-atoms on a 10 K carbonaceous surface is shown. (Right) The addition of H_2O molecules is illustrated. Note that the formation of carbonaceous layers is due to the high sticking of C-atoms and available flux. The angles of deposition are arbitrarily displayed.

The RAIR spectra reflecting the experiments of 1.1-1.3 and 2.1-2.3 in Table 3.1 are displayed in Figure 3.2. The left and right panels unambiguously confirm CH_4 formation by featuring the very strong ν_4 mode of CH_4 (Chapados & Cabana 1972) at various deposition times. Extra confirmation of CH_4 formation by D-isotope substitution and appearance of the ν_3 mode are provided in the Supporting Information, Figure S2. In both, C + H and C + H + H_2O experimental sets, CH_4 formation is observed within minutes, in addition to no detection of CH_n radicals or their recombination products such as C_2H_2, C_2H_4, and C_2H_6. This is consistent with the efficient recombinations between CH_n radicals and H-atoms, and that the lifetime of such radicals is relatively short under our experimental conditions. This also implies that the competing H-abstraction reactions do not dominate in either case. The abstraction reactions, CH + H $\rightarrow$ C + H_2 and CH_2 + H $\rightarrow$ CH + H_2, are reported to be essentially barrierless (Baulch et al. 1992; Harding et al. 1993), whereas the barrier for CH_3 + H $\rightarrow$ CH_2 + H_2 is reported to have a high value of ~7600-7700 K (Baulch et al. 1992). CH_4 + H $\rightarrow$ CH_3 + H_2 also has a high barrier height of ~7450-7750

Table 3.1: A list of experiments, along with the experimental parameters and subsequent product yields. Note that experiments 1.1-1.3 represent the same experiment, but with varying fluences (also with experiments 2.1-2.3). (-) and (<) refer to not applicable and non-detections, respectively. (*) Cannot directly compare to CH_4 column densities. See main text for more details. Details on band strength determination for column density calculations are found in the Methods section. The reported CH_4 column densities are overestimated by $< 25\%$, as C can possibly react with H_2/D_2 in the H_2O/D_2O experiments to form CH_4/CD_4, but not with H_2O/D_2O, as further discussed in the Supporting Information (see Figures S1 and S3).

No.	Experiments	T_{sample} (K)	Column density$_{CH_4/CD_4}$ (molecules cm^{-2})	Column density$_{H_2O}$ (molecules cm^{-2})	Ratio$_{CH_4:H_2O}$ (%)	Time (s)
1.1	C + H	10	2.8×10^{14}	-	-	1440
1.2	C + H	10	2.5×10^{14}	-	-	1080
1.3	C + H	10	2.1×10^{14}	-	-	720
2.1	C + H + H_2O	10	8.1×10^{14}	8.0×10^{15}	10	1440
2.2	C + H + H_2O	10	6.4×10^{14}	6.4×10^{15}	10	1080
2.3	C + H + H_2O	10	4.3×10^{14}	4.2×10^{15}	10	720
2.4	C + H_2 + H_2O	10	2.0×10^{14}	4.1×10^{15}	5	1440
3	C + D + H_2O	10	7.7×10^{14}*	7.6×10^{15}	10	1440
4	C + H + H_2O	25	$< 4.2 \times 10^{13}$	7.2×10^{15}	< 0.6	1440

K (Corchado et al. 2009), and thus may explain why CH_4 continues to form despite some abstraction reactions competing with addition reactions.

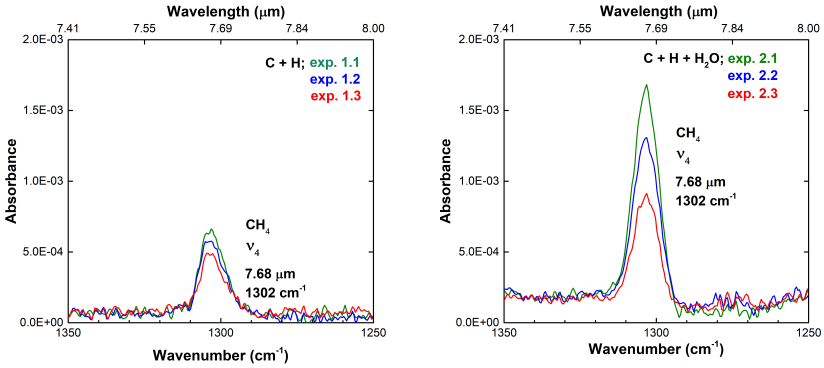

Figure 3.2: (Left) RAIR spectra, in which only the selected feature of interest is shown (i.e., CH_4 ν_4 mode), were acquired after co-deposition of C + H on a 10 K surface in 360 second intervals (exps. 1.1-1.3), and (right) after co-deposition of C + H + H_2O on a 10 K surface in 360 second intervals (exps. 2.1-2.3). RAIR spectra are offset for clarity.

It is apparent from Table 3.1 and the panels of Figure 3.2 that CH_4 formation is more efficient in the C + H + H_2O experiment. The formation rate of CH_4 in the C + H experiment is no greater than 3.5×10^{11} molecules cm^{-2} s^{-1}, and in the C + H + H_2O experiment, it is 5.6×10^{11} molecules cm^{-2} s^{-1}. Note that the total C + H kinetic curve (until CH_4 saturation) is non-linear. After

1440 s of deposition, the total column density of CH_4 amounts to 2.8×10^{14} molecules cm^{-2} and 8.1×10^{14} molecules cm^{-2} for the C + H and C + H + H_2O experiments, respectively. Thus, despite the H_2O-ice matrix, which could potentially block C- and H-atoms from meeting each other, formation of CH_4 is actually enhanced when H_2O is included. This phenomenon is likely, in part, due to the increase in the sticking coefficient of atomic H when H is in the presence of amorphous solid water (ASW) (Öberg et al. 2010; Veeraghattam et al. 2014), and the increase in the surface area that atoms can stick to (Mayer & Pletzer 1986). The sticking probability of H-atoms with an incident energy of 300 K on a 10 K ASW ice is 0.4 (Veeraghattam et al. 2014), in comparison to the lower value of ~0.02 for that of graphite (Lepetit et al. 2011). Note that the carbon allotrope formed from the atomic source is determined to be amorphous (Albar et al. 2017), and thus the sticking coefficient of H on our carbon surface is likely higher than ~0.02.

The surface formation mechanism is probed in the C + H + H_2O experiment at 25 K (exp. 4, Figure S4 of the Supporting Information). The formation of CH_4 at a deposition temperature of 25 K is negligible in comparison to the formation of CH_4 in exp. 2.1, and additionally the CH_4 feature is within the level of the noise. This finding indicates that the temperature of the surface largely influences the reaction probability, as the residence time of H-atoms drastically drops above ~15 K (Fuchs et al. 2009; Ioppolo et al. 2010; Chuang et al. 2016). Thus, the Langmuir-Hinshelwood mechanism, which is temperature dependent, is predominant in the formation of CH_4 at 10 K.

3.3 Astrochemical implications and conclusions

With the utilization of a UHV setup designed, in part, to investigate the simultaneous accretion of C- and H-atoms in two interstellar relevant ices, we experimentally confirm that CH_4 formation proceeds and is more favored when H_2O is added to the C + H reaction at 10 K. This supports the conclusions of the observational survey of CH_4 ice by Öberg et al. (2008) that much of the detected CH_4 is found in the polar phase of ice evolution and formed by atomic C and H. The main route to CH_4 formation in our experiments is H-atom addition to C-atoms in a H_2O ice:

$$C + H \underset{H_2O}{\rightarrow} CH, CH + H \underset{H_2O}{\rightarrow} CH_2, CH_2 + H \underset{H_2O}{\rightarrow} CH_3, CH_3 + H \underset{H_2O}{\rightarrow} CH_4$$

which predominantly follows a Langmuir-Hinshelwood mechanism at 10 K.

The findings presented here parallel the assumption used in models that the sequential hydrogenation of C is barrierless. It is suggested that astrochemical models take into account that the formation of interstellar CH_4 should still proceed when C and H accrete onto the growing polar ice, as it is experimentally shown that H_2O enhances the probability for C and H to react. Whether the CH_4 abundance will substantially increase due to the presence of H_2O on an interstellar dust grain needs to be tested in a model. As the astronomically observed CH_4-H_2O correlation towards YSOs is predominantly set by the availability of the simultaneous accretion of C, O, and H, the CH_4 formation rate factor of 2 in a H_2O-rich ice experiment is not expected to directly lead to a

CH_4 formation rate factor of 2 in an astrochemical model. Additionally, in an interstellar ice, C will compete with other species to react with H. Thus, it is also suggested that the assumed rate of 2×10^{11} s^{-1} used in models for barrierless reactions (*private communication, H. Cuppen*) should be multiplied by $1 < x < 2$ for CH_4 formation in a H_2O-rich ice by the sequential hydrogenation of C.

This work shows that CH_4 can be formed in the solid-state under conditions relevant to interstellar clouds, without the need for extra heat or 'energetic' particles. On the other hand, UV photons (or enhanced cosmic rays) are needed to maintain a high abundance of atomic C and O in the gas-phase, which can accrete onto grains to make CH_4 and H_2O ices. Thus, the early low density translucent cloud phase is optimally suited to make both ices simultaneously and abundantly. In the later denser cloud phases, most gaseous carbon has been transformed into CO, which – after freeze-out onto the grains – can be transformed into complex organic ices, and, under cold protoplanetary disk conditions, ultimately to CH_4 and hydrocarbon ices (Bosman et al. 2018). It is clear that the reaction proceeds effectively at lower versus higher temperatures, and is enhanced in a H_2O matrix, both of which are in-line with astronomical observations. Astrochemical modeling is necessary to take into account the available C-atom fluxes in the ISM in order to place the present findings into a cosmochemical picture. Such dedicated models can then be used to aid in the interpretation of CH_4 ice observations with the upcoming James Webb Space Telescope (JWST), as CH_4 is best observed with space-based observatories. The increase in sensitivity of the JWST Mid-Infrared Instrument is expected to allow observations of CH_4 ice towards numerous background stars to probe more quiescent environments, in addition to observations towards YSOs. The work presented here is the first experimental proof of solid-state CH_4 formed in a polar ice. The incorporation of a pure C-atom channel in interstellar networks is as important as including the N-atom channel for the formation of NH_3 (Fedoseev et al. 2014) and the O-atom channel for the formation of H_2O (Ioppolo et al. 2008). As molecular clouds are the universal starting point in the star and planet formation process, this also means that much of the chemical inventory in protoplanetary disks and possibly planets is due to the chemical processes that take place on icy dust grains in molecular clouds prior to collapse.

The present approach also has applications beyond the formation of CH_4. It becomes possible to focus on COM formation through C-atom addition (Charnley 1997a, 2001a; Charnley & Rodgers 2005, 2009). The carbon backbone of COMs has already been proven to be formed by the reaction between C-bearing radicals, such as between HCO and CH_2OH (Chuang et al. 2016). This new experimental way of forming COMs by adding atomic C will aid in better understanding the origin of detected COMs, as astrochemical models will be able to take into account the relevance of C-atom addition reactions by including data from experimental simulations, such as those found here.

3.4 Methods

The experiments presented in this article were performed with SURFRESIDE^2, which is an ultrahigh vacuum (UHV) apparatus that allows qualitative and quantitative investigations of the ice chemistry of molecular clouds. The initial design is discussed in the work by Ioppolo et al. (2013), and details on the recent modifications are provided by Qasim et al. (2019). The apparatus partially consists of three atomic beam line chambers that are connected to a main chamber, which reaches a base pressure of $2-3\times10^{-10}$ mbar prior to co-deposition. Within the middle of the chamber is a closed-cycle helium cryostat that has a gold-plated copper sample used to grow ices. On top of the sample lies a coating of carbon that is visible to the naked eye, and has been characterized to be amorphous when originating from the atomic carbon source (Albar et al. 2017). Due to the high sticking coefficient of atomic carbon, formation of these carbonaceous layers is difficult to avoid. Resistive heating of a cartridge heater was applied to heat the sample. With the incorporation of a sapphire rod, the sample is able to be cooled to a low temperature of 7 K and heated to a high temperature of 450 K. Such temperatures were measured by a silicon diode sensor that has an absolute accuracy of 0.5 K.

In this study, two of the three atomic beam lines were used to create atoms, where the base pressure of both atomic chambers was $2-3\times10^{-9}$ mbar. A Microwave Atom Source (MWAS; Oxford Scientific Ltd.), which consists of a 2.45 GHz microwave power supply (Sairem) that was operated at 200 W, was employed to produce H- and D-atoms from H_2 and D_2, respectively, with a dissociation rate that is less than unity. A nose-shaped quartz tube is attached at the exit of the source so that atoms can depart energy through collisions with the tube before reaching the cooled sample. An atomic carbon sublimation source (SUKO-A 40; Dr. Eberl MBE-Komponenten GmbH), which uses a power supply (Delta Elektronika, SM 15-100) to induce carbon sublimation, was exploited to create ground state C-atoms. Graphite powder was packed within a tantalum tube that was heated to around 2300 K, which leads to a reaction between molecular carbon and tantalum to form TaC_x. This process ultimately breaks apart molecular carbon into atomic carbon. Due to the high sticking coefficient of atomic carbon, a quartz pipe was not incorporated to cool the atoms prior to deposition. However, the heat of the C-atoms involved in the initial step of CH_4 formation is not expected to qualitatively affect the results, as C + H is expected to be barrierless, and C + H_2 $\rightarrow$ CH + H is highly endothermic (Harding et al. 1993; Guadagnini & Schatz 1996). The third atomic beam line, a Hydrogen Atom Beam Source (HABS) (Tschersich & Von Bonin 1998; Tschersich 2000; Tschersich et al. 2008), was not used as a source of H-atoms in this work.

Details on the preparation of gases and liquids used to create the interstellar ice analogues are described below. H_2 (Linde 5.0) and D_2 (Sigma-Aldrich 99.96%) gases were transferred into the MWAS vacuum chamber. A H_2O sample was connected to the HABS chamber, where the H_2O was cleaned before every experiment by one freeze-pump-thaw cycle. Note that H_2O was not formed on the surface but instead deposited, as the focus is to disentangle the formation routes to CH_4. All prepared gases and liquids were released into the main chamber by leak valves.

The reflection-absorption infrared spectroscopy (RAIRS) technique was performed to probe product formation *in situ*, as well as obtain quantitative information about the products formed through analysis of their vibrational modes. A Fourier Transform Infrared Spectrometer (FTIR), with a fixed scan range of 4000 - 700 cm^{-1} and resolution of 1 cm^{-1}, was applied in the RAIRS study. To measure the abundances of CH_4/CD_4 formed and the CH_4/CD_4:H_2O ice abundance ratios, a modified Lambert-Beer equation was used. Band strength values of 4.40×10^{-17} cm molecule^{-1}, 2.20×10^{-17} cm molecule^{-1}, and 4.95×10^{-17} cm molecule^{-1} were used to calculate the column densities of CH_4 (ν_4 mode; 1302 cm^{-1}), CD_4 (ν_4 mode; 993 cm^{-1}), and H_2O (ν_2 mode; 1665 cm^{-1}), respectively. The initial values were obtained from Bouilloud et al. (2015) for CH_4 and H_2O, and from Addepalli & Rao (1976) for CD_4. A transmission-to-RAIR setup determined proportionality factor of 5.5 was then applied. The proportionality factor was calculated using the band strength of CO (2142 cm^{-1}) measured on our setup through the laser interference technique, where the band strength is reported in Chuang et al. (2018).

To secure that the CH_4 formation rate is higher in the H_2O-rich experiment, the repeatability of the C + H and C + H + H_2O experiments was evaluated. As the formation rates are determined by plotting the CH_4 column densities as a function of time, the uncertainty in the formation rates and column densities can be assessed by measuring the relative standard deviation (RSD) between data points of the same experiment that was performed on different days. For the C + H and C + H + H_2O experiments, average RSD values of 10% and 2% were measured, respectively. Such values further secure the claim that the CH_4 formation rate is larger in a H_2O-rich ice. The higher repeatability of the C + H + H_2O experiment is predominantly due to the more accurate column density measurement of CH_4, as the S/N of the 1302 cm^{-1} feature is greater.

S1 Supporting Information

Figure S1 shows RAIR spectra in the range of 1350 - 1250 cm^{-1} in order to compare the control experiment of C + H_2 + H_2O with C + H(H_2) + H_2O, as not all of the H_2 is converted into H in the MW source. Thus, atomic C may participate in a sequence of reactions involving H_2 to ultimately form CH_4. As both experiments were performed under the same parameters (flux, deposition time, and temperature), the abundances of CH_4 formed can be compared. The column densities of CH_4 in the C + H(H_2) + H_2O and C + H_2 + H_2O experiments are 8.1×10^{14} molecules cm^{-2} and 2.0×10^{14} molecules cm^{-2}, respectively. This implies that the upper limit for the C + H_2 reaction route contribution towards the total CH_4 abundance is 25%. It is less because the more dominant reaction route, C + H, is omitted in the C + H_2 + H_2O experiment (i.e., the reaction efficiency is at least a factor of 4 less and likely much more). It is reported that C + H_2 barrierlessly leads to CH + H through the intermediate, CH_2, although it is endothermic by ~13,450 K (Harding et al. 1993; Guadagnini & Schatz 1996), and therefore considered negligible in the presented experiments. Thus, it is expected that the minor amount of CH_4 formed starting from H_2 is at least due to the barrierless reaction of C + H_2 to form the intermediate, CH_2, followed by two H-atom additions. CH_2 is stabilized due to the presence of the surface

third body. The barrier for the $CH_2 + H_2 \rightarrow CH_3 + H$ reaction is ambiguous (Gesser & Steacie 1956; Lu et al. 2010).

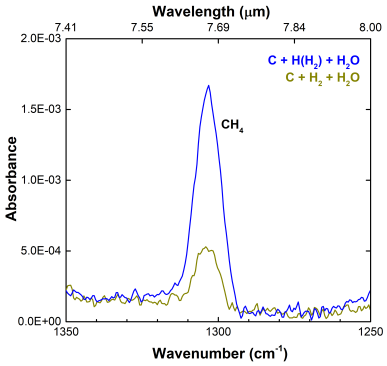

Figure S1: RAIR spectrum acquired after co-deposition of C + $H(H_2)$ + H_2O (exp. 2.1; blue) and C + H_2 + H_2O (exp. 2.4; green) on a 10 K surface, which shows the minor formation of CH_4 starting from H_2 versus H. RAIR spectra are offset for clarity.

Figure S2 provides additional proof for CH_4 formation in the C + H + H_2O experiments. The left panel shows the isotopic shift of the deformation mode when H-atoms are substituted by D-atoms in the co-deposition experiment. This additionally shows that CD_4 can also be formed in a H_2O-rich ice via atom-atom reactions, if D-atoms are available for reaction. A CD_4 column density of 7.7×10^{14} molecules cm^{-2} was measured, which is close to the CH_4 column density. However, the abundances cannot be directly compared, as the D-atom flux used was approximately twice less in comparison to that of H-atoms. The right panel shows the strong C-H stretching vibrational mode of CH_4.

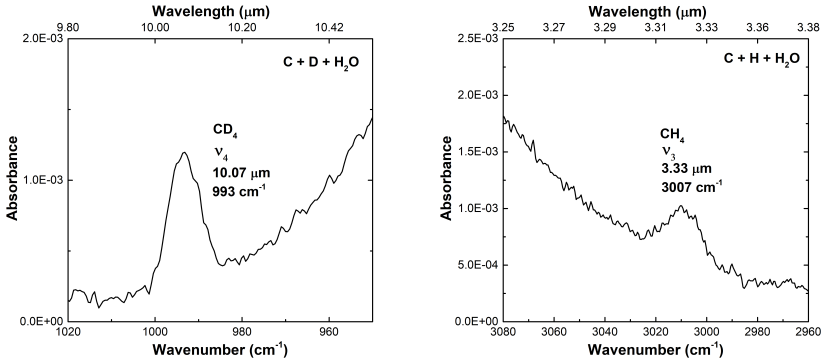

Figure S2: The two panels display proof of methane formation. (Left) The ν_4 mode in the C + D + H_2O experiment (exp. 3), which is intrinsic to that of CD_4 (Chapados & Cabana 1972). This is evidence for CH_4 formation in the C + H + H_2O experiment by observation of the isotopic shift. (Right) Evidence of CH_4 formation in the C + H + H_2O experiment (exp. 2.1) by observation of the CH_4 ν_3 mode on the H_2O wing. RAIR spectra are offset for clarity.

The absence of the CH_4 signature at ~1300 cm^{-1} in the C + D + H_2O experiment (exp. 3) is shown in Figure S3. This indicates that C and H_2O do not react to form CH_4 in exp. 3, and therefore should not contribute to form CH_4 by abstraction of H-atoms from H_2O. This is expected, as the competing reaction of atomic C and H(D) addition is likely barrierless. CD_3H, CD_2H_2, and CDH_3 were also not identified. Whether C reacts with the O-atom of H_2O will be investigated in a separate dedicated study. Figure S4 clearly shows that CH_4 formation is negligible at a deposition temperature of 25 K due to the drop in the H-atom residence time on the surface. This extended residence time required for CH_4 formation is an indication that both, H-atoms and CH_n intermediates have a period of time available to thermalize with the surface prior to reaction in the 10 K experiments.

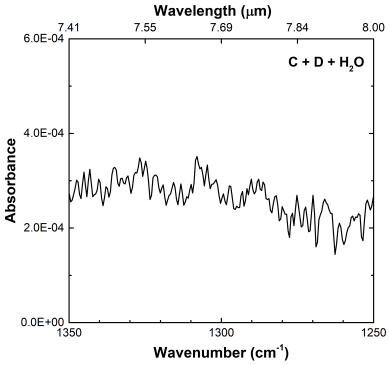

Figure S3: Lack of the C-H bending vibrational signal in the C + D + H_2O experiment (exp. 3), which shows that C does not react with H_2O to form CH_4. RAIR spectrum is offset for clarity.

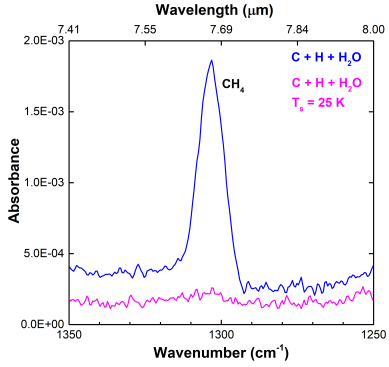

Figure S4: RAIR spectra acquired after co-deposition of C + H + H_2O on a 10 K surface (exp. 2.1; blue) and co-deposition of C + H + H_2O on a 25 K surface (exp. 4; pink), which shows the negligible formation of CH_4 at 25 K. RAIR spectra are offset for clarity.

Bibliography

Addepalli, V. & Rao, N. R. 1976, Indian J. Pure Appl. Phys., 14, 117
Aikawa, Y., Wakelam, V., Garrod, R. T., & Herbst, E. 2008, Astrophys. J., 674, 984
Albar, J., Summerfield, A., Cheng, T. S., et al. 2017, Sci. Rep., 7, 6598
Bar-Nun, A., Litman, M., & Rappaport, M. 1980, Astron. Astrophys., 85, 197
Baulch, D., Cobos, C., Cox, R., et al. 1992, J. Phys. Chem. Ref. Data, 21, 411
Boogert, A., Gerakines, P. A., & Whittet, D. C. 2015, Annu. Rev. Astron. Astrophys., 53, 541
Bosman, A. D., Walsh, C., & van Dishoeck, E. F. 2018, Astron. Astrophys., 618, A182
Bouilloud, M., Fray, N., Bénilan, Y., et al. 2015, Mon. Not. R. Astron. Soc., 451, 2145
Chapados, C. & Cabana, A. 1972, Can. J. Chem., 50, 3521
Charnley, S. 1997a, in IAU Colloq. 161: Astronomical and Biochemical Origins and the Search for Life in the Universe, ed. C. Cosmovici, S. Bowyer, & D. Werthimer, Vol. 161, 89–96
Charnley, S. 2001a, in The bridge between the Big Bang and Biology: Stars, Planetary Systems, Atmospheres, Volcanoes: their Link to Life, ed. F. Giovannelli, 139–149
Charnley, S. & Rodgers, S. 2005, Proceedings of the International Astronomical Union, 1, 237
Charnley, S. & Rodgers, S. 2009, in Bioastronomy 2007: Molecules, Microbes and Extraterrestrial Life, ed. K. Meech, J. Keane, M. Mumma, J. Siefert, & D. Werthimer, Vol. 420, 29–34
Chuang, K.-J., Fedoseev, G., Ioppolo, S., van Dishoeck, E. F., & Linnartz, H. 2016, Mon. Not. R. Astron. Soc., 455, 1702
Chuang, K.-J., Fedoseev, G., Qasim, D., et al. 2018, Astrophys. J., 853, 1
Corchado, J. C., Bravo, J. L., & Espinosa-Garcia, J. 2009, J. Chem. Phys., 130, 184314
Cuppen, H., Walsh, C., Lamberts, T., et al. 2017, Space Sci. Rev., 212, 1
Fedoseev, G., Ioppolo, S., Zhao, D., Lamberts, T., & Linnartz, H. 2014, Mon. Not. R. Astron. Soc, 446, 439
Formisano, V., Atreya, S., Encrenaz, T., Ignatiev, N., & Giuranna, M. 2004, Science, 306, 1758
Fuchs, G., Cuppen, H., Ioppolo, S., et al. 2009, Astron. Astrophys., 505, 629
Gesser, H. & Steacie, E. 1956, Can. J. Chem., 34, 113
Gibb, E., Mumma, M., Russo, N. D., DiSanti, M., & Magee-Sauer, K. 2003, Icarus, 165, 391
Guadagnini, R. & Schatz, G. C. 1996, J. Phys. Chem., 100, 18944
Harding, L. B., Guadagnini, R., & Schatz, G. C. 1993, J. Phys. Chem., 97, 5472
Hiraoka, K., Miyagoshi, T., Takayama, T., Yamamoto, K., & Kihara, Y. 1998, Astrophys. J., 498, 710
Ioppolo, S., Cuppen, H., Romanzin, C., van Dishoeck, E. F., & Linnartz, H. 2008, Astrophys. J., 686, 1474
Ioppolo, S., Cuppen, H., Romanzin, C., van Dishoeck, E. F., & Linnartz, H. 2010, Phys. Chem. Chem. Phys., 12, 12065
Ioppolo, S., Fedoseev, G., Lamberts, T., Romanzin, C., & Linnartz, H. 2013, Rev. Sci. Instrum., 84, 1
Lepetit, B., Lemoine, D., Medina, Z., & Jackson, B. 2011, J. Chem. Phys., 134, 114705
Lu, K.-W., Matsui, H., Huang, C.-L., et al. 2010, J. Phys. Chem. A, 114, 5493
Mayer, E. & Pletzer, R. 1986, Nature, 319, 298
Mousis, O., Gautier, D., & Coustenis, A. 2002, Icarus, 159, 156
Mousis, O., Lunine, J. I., Pasek, M., et al. 2009, Icarus, 204, 749
Mumma, M. J., DiSanti, M. A., Russo, N. D., et al. 1996, Science, 272, 1310

Nuth III, J. A., Charnley, S. B., & Johnson, N. M. 2006, in Meteorites and the Early Solar System II, ed. D. Lauretta & H. McSween (this volume. Univ. of Arizona, Tucson), 147–167
Öberg, K. I., Boogert, A., Pontoppidan, K. M., et al. 2008, Astrophys. J., 678, 1032
Öberg, K. I., van Dishoeck, E. F., Linnartz, H., & Andersson, S. 2010, Astrophys. J., 718, 832
Qasim, D., Fedoseev, G., Lamberts, T., et al. 2019, ACS Earth Space Chem., 3, 986
Smith, I. W. 1989, Astrophys. J., 347, 282
Stern, S., Bagenal, F., Ennico, K., et al. 2015, Science, 350, aad1815
Swain, M. R., Vasisht, G., & Tinetti, G. 2008, Nature, 452, 329
Tschersich, K. 2000, J. Appl. Phys., 87, 2565
Tschersich, K., Fleischhauer, J., & Schuler, H. 2008, J. Appl. Phys., 104, 1
Tschersich, K. & Von Bonin, V. 1998, J. Appl. Phys., 84, 4065
Veeraghattam, V. K., Manrodt, K., Lewis, S. P., & Stancil, P. 2014, Astrophys. J., 790, 4